

$p(1\times 1)$ to $c(4\times 8)$ periodicity change in ultrathin iron silicide on Si(111)

S. Hajjar, G. Garreau, S. Pelletier, D. Bolmont, and C. Pirri*

Laboratoire de Physique et de Spectroscopie Electronique CNRS-UMR7014, Faculté des Sciences et Techniques, 4, rue des frères Lumière, 68093 Mulhouse, France

(Received 5 December 2002; revised manuscript received 26 March 2003; published 3 July 2003)

Iron silicide layers grown by solid phase epitaxy on Si(111) are investigated using scanning tunnel microscope (STM), low-energy electron diffraction and low-energy ion spectroscopy. These layers, which are flat and homogeneous for a selected Fe thickness range, exhibit a $p(2\times 2)$ surface superstructure whatever the annealing temperature above 600 K. Voltage-dependent STM images reveal a modification of the silicide symmetry, from a $p(1\times 1)$ towards a $c(4\times 8)$ in-plane periodicity, above 800 K. This transition is associated with an organization of chemical species under two Si atomic planes.

DOI: 10.1103/PhysRevB.68.033302

PACS number(s): 68.37.Ef, 68.49.Sf, 68.55.-a, 81.05.Je

The growth of iron silicides on silicon has been widely studied in the last decade. This interest was mainly driven by the formation of a semiconducting phase β -FeSi₂ in epitaxy on Si(111) or Si(100). A more recent interest is explained by the possible formation of magnetic layers, lines, or dots on Si. These magnetic materials could be integrated in micro-electronic devices. Nevertheless, one major obstacle to overcome is the uncontrolled reaction at the Fe/Si interface. The formation of a perfectly flat and defect-free disilicide layer at the Fe/Si interface is a possible way to control the chemistry at the Fe/Si interface. This could reduce the Si diffusion within the Fe layer, and also promote epitaxy. Numerous studies have been devoted to the growth of FeSi₂ on Si(111). FeSi₂ crystallizes in different phases, depending on the growth conditions. Their formation has been mainly studied using experimental techniques such as photoemission,¹⁻³ x-ray diffraction,⁴⁻⁷ low-energy electron diffraction (LEED),⁸⁻¹¹ x-ray photoelectron diffraction¹¹⁻¹⁵ and x-ray absorption.^{14,16} Nevertheless, thin iron silicide films generally present a mixture of phases. This makes their identification very difficult with the previous experimental tools. The FeSi₂/Si(111) interface has also been investigated by scanning tunneling microscopy (STM) measurements.^{10,17-22} These measurements have shown that the silicide surface is rather rough due to the formation of several concomitant phases.

In this Brief Report, we show that thin FeSi₂ layers can be formed by solid phase epitaxy, in either a CsCl-derived structure or a more ordered one, depending on the growth conditions. In particular, a flat and perfectly ordered phase, with an in-plane $c(4\times 8)$ periodic structure, is formed above 800 K. Both phases are studied by STM, LEED, and low-energy ion spectroscopy (LEIS).

The experimental setup is composed of three connected ultrahigh vacuum chambers equipped with LEIS, STM, LEED techniques and deposition facilities. The Si(111) samples (p type with a resistivity of about 0.1 Ω cm) were cleaned by repeated flashes at 1500 K at a pressure below 1×10^{-10} mbar. The silicide layers were grown by the deposition of an Fe layer, with a thickness between 1.6 and 2.2 ML (monolayer) onto the Si substrate maintained at room temperature from a homemade evaporator and postannealed

at a temperature in the 700–900 K range. The Fe deposition rate was about 0.3 ML per minute at a pressure of about 2×10^{-10} mbar. One Fe monolayer is defined as the atomic density of a Si(111) plane, i.e., 7.8×10^{14} atoms/cm². STM measurements were made in a room-temperature-operating microscope (commercial Omicron STM-AFM microscope), in the constant-current mode. Electrochemically etched, *in situ* cleaned tungsten tips were used. The LEIS measurements were performed with an incident beam of 1-keV He⁺ ions. The ions were analyzed using a hemispherical energy analyzer (150 mm in radius) and a 7 Channeltron multidection system. The scattering angle of the ions was 130° and the acceptance angle of the analyzer was set to $\pm 8^\circ$.

Figure 1(a) shows a large scale STM image of 1.7-ML Fe deposit postannealed at 700 K for 10 min. The silicide layer completely covers the Si(111) terraces and forms on two successive Si bilayers on a given Si(111) terrace. A detailed description of the silicide growth on Si(111) will be given in a forthcoming paper.²³ So, all features visible in Fig. 1(a) (terraces and islands) are composed of the same silicide. It exhibits a $p(2\times 2)$ LEED pattern (inset), as usually observed for thicker epitaxial FeSi_{1+x} silicide layers. The $p(2\times 2)$ surface periodicity has been associated with the segregation of 1/4 Si monolayer.^{12,17} Figure 1(b) shows an image, with atomic resolution, taken at a sample voltage of $V = +1.2$ V. The adatoms form a $p(2\times 2)$ network of protrusions, with a lattice parameter twice that of the unreconstructed Si(111) surface, in line with the LEED pattern. The most striking feature is that protrusions with different brightness levels are observed. Note that at a given sample voltage, the image contrast strongly depends on the tip quality. In some cases, this additional contrast is very hard to observe. Nevertheless, these intensity variations can be seen over a very large sample voltage range for most tips we have used. Similar STM contrasts have already been observed for other Si-based systems.²⁴⁻²⁷ In the present work, the surface network is made of a $p(2\times 2)$ array of adatoms and the difference in the protrusion brightness is not due to missing adatoms.

Annealing the silicide layer above 800 K induces drastic modifications in the silicide crystallographic structure. Figure 2(a) shows a large scale STM image after annealing the silicide at 900 K for 1 h. The silicide layer is still perfectly

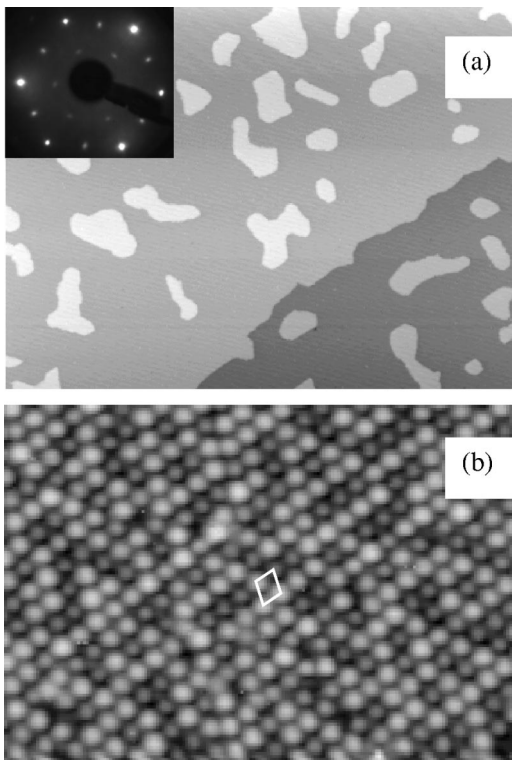


FIG. 1. Empty-state ($V_s = +1.2$ V, $I_t = 0.1$ nA) STM images measured after the reaction of 1.7 Fe monolayers on Si(111) by annealing at 700 K. (a) (400 nm \times 240 nm) image, (b) high-resolution image (19 nm \times 13 nm) showing protrusions with different brightness. The parallelogram in (b) indicates the $p(2 \times 2)$ unit cell of atoms in the topmost layer. Inset: LEED pattern taken at a primary electron energy $E = 53$ eV.

flat, for an annealing temperature at which thicker layers exhibit three-dimensional islands. The silicide surface exhibits several domains, separated by white lines in Fig. 2(a) and visualized thanks to spectroscopic effects at the domain boundaries. A detail of the atomic surface structure, collected at a positive sample voltage $V = +1.2$ V, is displayed in Fig. 2(b). The surface periodicity is still $p(2 \times 2)$ but mainly two types of protrusion are observed, called bright and dark. The bright and dark protrusions are now ordered in a $c(4 \times 8)$ network. As for the low-temperature annealed layers, this contrast is hard to detect in some cases, showing that the silicide surface is still completely covered by a $p(2 \times 2)$ array of adatoms. The $c(4 \times 8)$ domains are oriented in three equivalent orientations, rotated each other by 120° , which reflect in the $c(4 \times 8)$ LEED pattern shown as inset in Fig. 2(a). Furthermore, the image in Fig. 2(b) reveals the formation of out-of-phase domains whose boundary limit is indicated by an arrow. These out-of-phase domains are associated with the accommodation of adatoms in equivalent surface sites, since similar domains are observed in Fig. 1(b).

The most interesting feature here is the ordering of the bright and dark protrusions upon annealing at 900 K, which could be associated with a radical change in the silicide structure symmetry, from a $p(1 \times 1)$ to a $c(4 \times 8)$. The different contrasts in Figs. 1 and 2 could originate from topographic effects—atoms with different vertical position, from

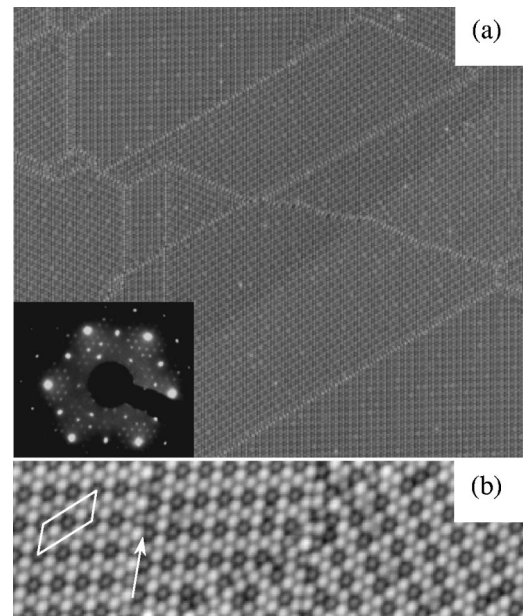


FIG. 2. Empty-state ($V_s = +1.2$ V, $I_t = 0.1$ nA) STM images measured after the reaction of 1.7 Fe monolayers on Si(111) by annealing at 900 K. (a) (100 nm \times 70 nm) image, (b) high-resolution image (28 nm \times 8 nm) showing protrusions with different brightness. The parallelogram in (b) indicates the $c(4 \times 8)$ periodicity. Inset: LEED pattern taken at a primary electron energy $E = 53$ eV.

spectroscopic effects—local density of states, or even from a mixture of both effects. The spectroscopic origin of the different site brightness is clearly evidenced by the drastic change in the image contrast upon changing the amplitude or the sign of the sample voltage. Figure 3 shows STM images taken on a silicide layer annealed at 700 K [(a) and (b)] and 900 K [(c) and (d)] for $V = +1.9$ V [(a) and (c)] and $V = -1.9$ V [(b) and (d)], respectively. In this figure, the brightest spot at a given voltage becomes the darkest at the

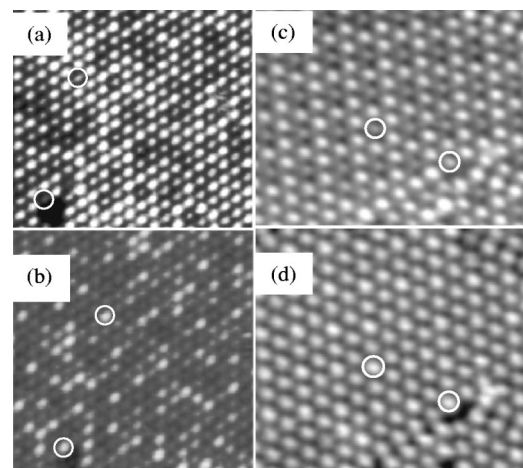


FIG. 3. Empty-state ($V_s = +1.9$ V) (a,c) and filled-state ($V_s = -1.9$ V) (b,d) STM images collected after the reaction of 1.7 Fe monolayers on Si(111) by annealing at 700 K (a,b) and 900 K (c,d). The open circles are located on the same atomic sites for each sample.

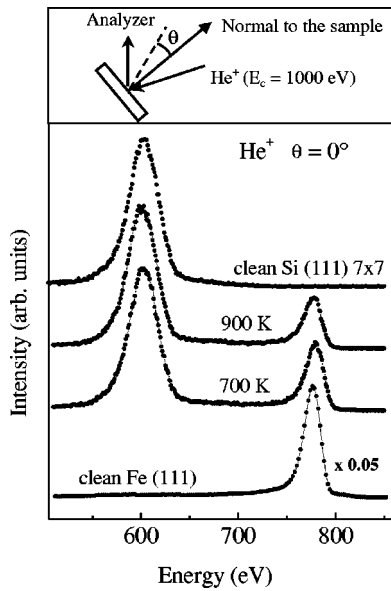


FIG. 4. (a) Yield of scattered He^+ ions versus kinetic energy collected from clean Fe(111), clean Si(111) 7×7 , 1.7 Fe monolayers annealed at 700 K and 900 K. The primary energy of the ions is 1000 eV.

opposite one. Note that it is very difficult to see the contrast for the negative sample polarities.

Thin Fe silicides grown by solid phase epitaxy below 800 K are known to crystallize in a defect-CsCl FeSi_{1+x} structure.¹ This structure is derived from a metastable CsCl-FeSi one by the formation of randomly distributed Fe vacancies, as first proposed by von Känel *et al.*¹ These vacancies should modify the local density of states above some surface adatoms and thus reflect in the atomically resolved image as spots with different brightness, as suggested by Siringhaus *et al.*²⁰ Nevertheless, the difference in protrusion brightness could alternatively be attributed to Si atoms in substitution on Fe sites, as proposed by Jedrecy *et al.*⁶ and/or to Fe and Si sites in the topmost layer, as observed for other metal/Si(111) systems.^{24,25,27} In that respect, we have performed LEIS, which gives the chemical composition of the outermost layers. Figure 4 shows LEIS spectra recorded on silicide layers for a 1.7-ML Fe deposit postannealed at 700 K and 900 K. This figure also includes LEIS spectra recorded on clean Si(111) 7×7 and on a pure Fe(111) layer, which are used as reference compounds. The Fe peak, located at 776 eV, is very small compared to that of pure Fe while the Si one, located at 600 eV, is as high as that of clean Si. A comparison of the Fe to Si peak intensity ratio with the Co to Si one obtained for $\text{CoSi}_2(111)$ (Ref. 28) indicates that the Fe silicide layers are terminated by more than one Si-rich layer. Note that the LEIS spectra include the contribution of the inner Si and Fe layers, which could be more or less visible, depending on the surface crystallography. The Fe plane that mainly contributes to the LEIS spectra is obtained from the angular dependence of the LEIS spectra.

Figure 5 shows the Fe and Si yields versus polar angle θ along the $[10-1]$ direction of the silicon crystal. Both Fe and Si yields are corrected for sample area effects. The Si yield is

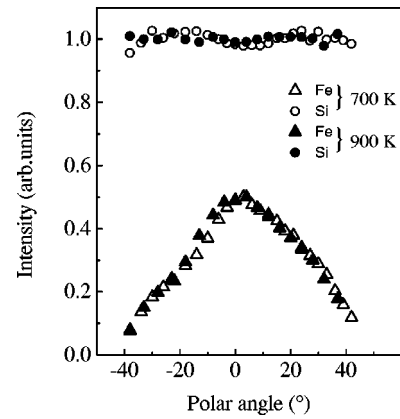


FIG. 5. Plot of Fe and Si yield versus polar angle θ for a 1.7 Fe monolayer deposit annealed at 700 K and 900 K. These polar profiles were measured along the $[10-1]$ crystallographic direction of the Si(111) substrate.

found to be constant versus polar angle, showing that its contribution arises mainly from the topmost silicide layer. In contrast, the Fe contribution to LEIS spectra shows a pronounced maximum at $\theta=0^\circ$ and strongly decreases for both positive (increasing the angle of incidence of He^+ ions) and negative (increasing the angle of detection of backscattered He^+ ions) polar angles. Almost the same bell-shaped curves are measured along the $\{1-21\}$ directions of the Si crystal. This clearly shows that He^+ ions impinge Fe sites at $\theta=0$. For both azimuthal directions, the Fe signal is shadowed upon increasing $|\theta|$, showing that the Fe atoms which contribute to the LEIS signal are below one or more Si top layers. In that respect, the comparison of these spectra with that measured on $\text{CoSi}_2(111)$ (Ref. 28) is helpful. Indeed, a similar behavior of Fe yield versus polar angle is observed on $\text{CoSi}_2(111)$, which is known to be terminated by only one Si top layer. The main difference resides in a metal to Si ratio lower in the present experiments. This is probably due to the presence of additional Si atoms, named adatoms. These Si adatoms could lie in different surface sites but they are expected to reduce the Fe contribution to the LEIS signal in both cases. The Si amount is estimated from that measured on $\text{CoSi}_2(111)$. LEIS measurements are thus consistent with a silicide surface terminated by a first adatom plane $[1/4$ of a monolayer which induces the $p(2 \times 2)$ surface superstructure] on top of a complete Si plane. These measurements show that the difference in STM protrusion intensity can safely be associated with a local change in density of states close to the Fermi level, i.e., spectroscopic effects, arising from the formation of Fe vacancies and/or Si substitution on the Fe sites.

Therefore, the contrast modification in STM images versus annealing temperature could be relevant to a structural transformation. The silicide achieved at 700 K has a cubic structure, of Fe-defected CsCl-FeSi type, as already observed for a low-temperature anneal.²⁰ The STM images taken on the silicide layer annealed at 900 K exhibit an additional $c(4 \times 8)$ surface modulation. This suggests that the silicide structure could be of a tetragonal symmetry, with a vacancy

arrangement close to that found in thicker Fe silicide layers.^{4–6} This thin silicide layer, formed upon annealing 1.6–2.2 Fe monolayers above 800 K, could be a precursor layer of the thicker α -type FeSi₂ layers. This is in line with the observation of such $c(4\times 8)$ contrast in STM images for very low Fe deposits only. The STM images are quite different for a higher Fe coverage, whatever the annealing temperature.²³

In conclusion, perfectly flat Fe-silicide layers are formed at very low Fe deposits (between 1.6 and 2.2 ML) on Si(111), with either a $p(1\times 1)$ or a $c(4\times 8)$ lattice periodicity. A silicide with a $p(1\times 1)$ periodicity is achieved at low

annealing temperature (600–800 K). This silicide transforms above 800 K and has a $c(4\times 8)$ periodicity. Both silicides are terminated by one $p(2\times 2)$ reconstructed Si adatom plane on top of a Si plane. Owing to the formation of Fe vacancies upon annealing a metastable CsCl-type FeSi silicide on Si(111), the symmetry change observed by STM could result from a rearrangement of Fe vacancies within the buried Fe layers. The $c(4\times 8)$ silicide is of very high quality: it is homogeneous, covers the whole Si substrate, and is thermally stable up to about 900 K. It appears, therefore, as an optimal template for the growth of well-controlled layers, magnetic for instance, on top of it.

*Corresponding author. Email address: c.pirri@uha.fr

- ¹H. von Känel, K.A. Mäder, E. Müller, N. Onda, and H. Sirringhaus, *Phys. Rev. B* **45**, 13 807 (1992).
- ²J. Alvarez, A.L. Vasquez de Parga, J.J. Hinarejos, J. de la Figuera, E.G. Michel, C. Ocal, and R. Miranda, *J. Vac. Sci. Technol. A* **11**, 929 (1993).
- ³U. Kafader, C. Pirri, P. Wetzel, and G. Gewinner, *Appl. Surf. Sci.* **64**, 297 (1993).
- ⁴J. Chevrier, P. Stocker, Le Thanh Vinh, J.M. Gay, and J. Derrien, *Europhys. Lett.* **22**, 449 (1993).
- ⁵K.L. Whiteaker, I.K. Robinson, C. Benson, D.M. Smilgies, N. Onda, and H. von Känel, *Phys. Rev. B* **51**, 9715 (1995).
- ⁶N. Jedrecy, A. Waldhauer, M. Sauvage-Simkin, R. Pinchaux, and Y. Zheng, *Phys. Rev. B* **49**, 4725 (1994).
- ⁷M. Sauvage-Simkin, N. Jedrecy, A. Waldhauer, and R. Pinchaux, *Physica B* **198**, 48 (1994).
- ⁸X. Wallart, J.P. Nys, and C. Tételin, *Phys. Rev. B* **49**, 5714 (1994).
- ⁹S. Hong, U. Kafader, P. Wetzel, G. Gewinner, and C. Pirri, *Phys. Rev. B* **51**, 17 667 (1995).
- ¹⁰A.L. Vasquez de Parga, J. de la Figuera, C. Ocal, and R. Miranda, *Ultramicroscopy* **42–44**, 845 (1992).
- ¹¹U. Starke, W. Weiss, M. Kutschera, R. Bandorf, and K. Heinz, *J. Appl. Phys.* **91**, 6154 (2002).
- ¹²A.L. Vasquez de Parga, J. de la Figuera, C. Ocal, and R. Miranda, *Europhys. Lett.* **18**, 595 (1992).
- ¹³S. Hong, P. Wetzel, D. Bolmont, G. Gewinner, and C. Pirri, *J. Appl. Phys.* **78**, 5404 (1995).
- ¹⁴U. Kafader, M.H. Tuilier, C. Pirri, P. Wetzel, G. Gewinner, D. Bolmont, O. Heckmann, D. Chandesris, and H. Magnan, *Europhys. Lett.* **22**, 529 (1993).
- ¹⁵A. Mascaraque, J. Avila, C. Teodorescu, M.C. Asensio, and E.G. Michel, *Phys. Rev. B* **55**, R7315 (1997).
- ¹⁶C. Pirri, M.H. Tuilier, P. Wetzel, S. Hong, D. Bolmont, G. Gewinner, R. Cortès, O. Heckmann, and H. von Känel, *Phys. Rev. B* **51**, 2302 (1995).
- ¹⁷W. Raunau, H. Niehus, T. Schilling, and G. Comsa, *Surf. Sci.* **286**, 203 (1993).
- ¹⁸J. Alvarez, A.L. Vasquez de Parga, J.J. Hinarejos, J. de la Figuera, E.G. Michel, C. Ocal, and R. Miranda, *Phys. Rev. B* **47**, 16 048 (1993).
- ¹⁹H. Sirringhaus, N. Onda, E. Müller-Gubler, P. Müller, St. Zehnder, and H. von Känel, *Surf. Sci.* **287/288**, 1019 (1993).
- ²⁰H. Sirringhaus, N. Onda, E. Müller-Gubler, P. Müller, R. Stalder, and H. von Känel, *Phys. Rev. B* **47**, 10 567 (1993).
- ²¹N. Motta, A. Sgarlata, G. Gaggiotti, F. Patella, A. Balzarotti, and M. De Crescenzi, *Surf. Sci.* **287**, 257 (1993).
- ²²N. Minami, D. Makino, T. Matsumura, C. Egawa, T. Sato, K. Ota, and S. Ino, *Surf. Sci.* **514**, 211 (2002).
- ²³S. Hajjar, G. Garreau, and C. Pirri (unpublished).
- ²⁴R.J. Hamers, *Phys. Rev. B* **40**, 1657 (1989).
- ²⁵J. Slezak, P. Mutombo, and V. Chab, *Phys. Rev. B* **60**, 13 328 (1999).
- ²⁶V.A. Gasparov, M. Riehl-Chudoba, B. Schröter, and W. Richter, *Europhys. Lett.* **51**, 527 (2000).
- ²⁷B. Voigtlander, V. Scheuch, H.P. Bonzel, S. Heinze, and S. Blügel, *Phys. Rev. B* **55**, R13 444 (1997).
- ²⁸S. Hong, P. Wetzel, G. Gewinner, and C. Pirri, *J. Vac. Sci. Technol. A* **14**, 3236 (1996).